INL/CON-23-75292-Revision-1

Steam Generator Model Design Parameter Sensitivity Study Using Advanced Optimization Tools

August 2024

Changing the World's Energy Future

Tejas Kedlaya, Congjian Wang, Piyush Sabharwall, Palash Kumar Bhowmik

Idaho National Laboratory

INL/CON-23-75292-Revision-1

Steam Generator Model Design Parameter Sensitivity Study Using Advanced Optimization Tools

Tejas Kedlaya, Congjian Wang, Piyush Sabharwall, Palash Kumar Bhowmik

August 2024

Idaho National Laboratory
Idaho Falls, Idaho 83415

http://www.inl.gov

Prepared for the
U.S. Department of Energy
Under DOE Idaho Operations Office
Contract DE-AC07-05ID14517

Steam Generator Model Design Parameter Sensitivity Study Using Advanced Optimization Tools

Palash K. Bhowmik[1]*, Tejas Kedlaya[2], Congjian Wang[1], and Piyush Sabharwall[1]

[1] Thermal Fluid Systems Methods and Analysis
Idaho National Laboratory
P.O. Box 1625, MS 3818
Idaho Falls, ID, USA 83415-3818
palashkumar.bhowmik@inl.gov; congjian.wang@inl.gov; piyush.sabharwall@inl.gov

[2]School of Nuclear Engineering
Purdue University
363 N Grant Street
West Lafayette, IN, USA 47907
tkedlaya@purdue.edu

ABSTRACT

This study focuses on design parameter sensitivity studies pertaining to a steam generator (SG) model, usi ng both Python and machine-learning tools. The SG model is a mathematical representation (including flu id flow and heat transfer equations/models/correlations) of a steam-generating unit in a pressurized water reactor (PWR)-type small modular reactor (SMR) system. Design studies involve changing the model's in put design parameters (e.g., temperature, pressure, mass flow rate) to observe the resulting effects on the output of the system (e.g., heat transfer coefficient [HTC], Nusselt number, heat transfer performance). Se nsitivity studies analyze the degree to which system output and/or desired parameters (e.g., HTC or heat tr ansfer performance) are sensitive to changes in input parameters. By using machine-learning tools such as the Risk Analysis Virtual Environment (RAVEN) developed at Idaho National Laboratory (INL), detailed design parametric sensitivity studies and model optimization were performed

. Six input parameters—namely, the pressure, temperature, and mass flow rate for the inlet of the primary-side (hot fluid) and secondary-side (cold fluid) of the SG—were randomly perturbed via RAVEN's Mont e Carlo Sampler module, using uniform distributions (±1% relative changes). The analysis results give val uable insights into SG system performance and optimization, and provide justification for researching opti mized sensor placement to effectively monitor and obtain experimental data.

KEYWORDS

steam generator (SG), sensitivity study, design optimization

1.0 INTRODUCTION

Recent modern innovations have led to the advancement of novel reactor technologies, many of which car ry the potential to greatly reduce carbon emissions while still maintaining safety and efficiency. Small mo dular reactors (SMRs) are one such technology, that promises small and modular capabilities, including e conomic and safety advantages for which SMRs have received increased attention recently [1][2].

Steam generators (SGs) in a reactor system—produce steam in secondary-side coolant by taking heat fro m the primary-side coolant—is one of the important component which requires details design analyses an

* Corresponding author email address: palashkumar.bhowmik@inl.gov

d experimentations to support reactor system design, analysis and licensing [3]. Steam then spins the turbi nes and converts the heat output from the power plant into usable electrical energy. The vertical, once-thr ough SG, which is the primary subject of this study, comes from a reference SMR design with passive saf ety features [4]. Reactor heat is fed into a hot fluid that enters the hot-leg (HL) through the riser section an d is then carried through the various small SG tubes. This is referred to as the primary-side. The secondar y-side consists of the shell encasing the SG tubes and provides a path along which the secondary fluid can flow, thus enabling heat transfer between the primary and secondary fluids to occur [5]. As this secondary fluid travels through the SG, it gains heat and eventually turns into dry, superheated steam.

As shown in **Figure 1**, the SG tubes are supported by baffles positioned within the shell where secondary fluid flows through. The middle column, or "riser," experiences a change in cross-sectional area, becomin g wider at the top. The hot fluid becomes gathered up at this point prior to being sent directly back down t hrough the SG tubes. Therefore, heat transfer occurs as the heat that is being generated moves between th e primary and secondary sides of the shell. Modeling the thermal-hydraulic performance of this system als o is important, as it is crucial to both reactor safety and normal operations that the SG is constantly remov ing heat from the reactor primary coolant as expected. It allows for a conceptual addition to computationa l fluid mechanics (CFD) modeling, as known correlations can be used so the results can be cross-checked according to the laws of physics.

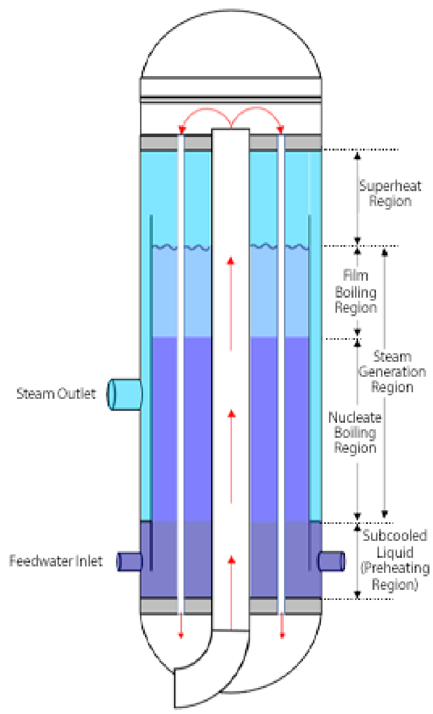

Figure 1: SMR once-through SG
(Taken from: https://holtecinternational.com/products-and-services/smr/, accessed August 10, 2023) [4].

The SG Python code is based on a series of iterative calculations. Figure 2 shows a schematic of the comp utational grid. The entire length of the SG is split into over a thousand small sections, with the fluid prope rties assumed to be constant in each. The initial outlet temperature is estimated, and then the input parame ters are used to find the boundary conditions for each consecutive interval. This enables spatial analysis of the thermodynamic data. The calculation loop is repeated across the entire length of the SG until the error between the estimated and calculated values becomes low enough for the code to be considered complete. The code also accounts for the phase changes in the secondary-side of the SG, which transitions from sub-cooled boiling, to nucleate boiling, to film boiling, and eventually, to superheated steam.

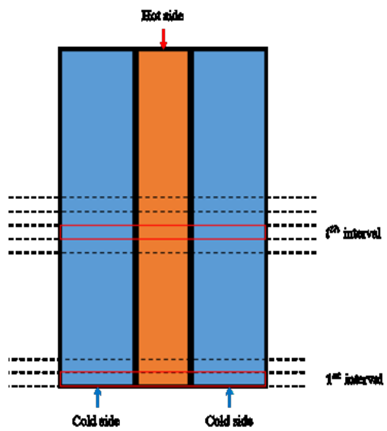

Figure 2: Python code computational grid schematic.

Python also presents advantages from a data analysis perspective, and because it is open source, it allows for integration with machine-learning (ML) platforms, such as the Risk Analysis Virtual Environment (R AVEN), which was developed by Idaho National Laboratory (INL) [6]. This allows for an artificial intelli gence (AI)-based approach to conducting a sensitivity analysis of the SG data.

The primary goal of this study is to perform a parametric and sensitivity analysis of the SG model. The pa rametric study will shed light on how tweaking each input parameter by a set amount changes the overall output in terms of the heat transfer coefficient (HTC) or the temperature and pressure profile. A sensitivit y analysis will reveal how each individual input parameter affects the overall HTC output. Tracking this s ensitivity spatially will give us a model that describes the local sensitivities of the SG to different paramet ers. This is important, as knowing where certain properties are sensitive to change can foster effective pla cement of sensors and related equipment. It then becomes possible to track SG sensitivity by manually ch anging the input parameters, and then applying RAVEN to run the code over and over again.

This sensitivity and parametric study can help identify regions in the length of the SG where certain para meters are more sensitive to change. This aids in strategically placing sensors to where they can most effe ctively monitor SG thermodynamic conditions [7] [8]. It also helps with stress testing the SG. Running thi s code over and over again helps determine the range over which the correlations used in the code remain viable. The RAVEN-based analysis also leaves room for more implementation in the future. With the sou rce code and RAVEN input file, it is possible to obtain more than just the SG sensitivity data. The capabil ities provided in RAVEN include anomaly detection and optimization to show the ideal input conditions f or SG operation. The RAVEN sensitivity analysis thus helps us obtain a more in-depth understanding of t he thermodynamic SG model.

2.0 STEAM GENERATOR MODEL

As mentioned earlier, the code operates by splitting the length of the SG into over a thousand intervals an d evaluating consecutive boundary conditions to determine the thermal-hydraulic properties. The code co nsiders both sub-cooled water and superheated steam. In scaled-down models, such as is the case with the SMR-160 half-height design used in our studies, the flow may transition from turbulent to laminar. Thus, the code accounts for laminar, transitional, and turbulent flow regimes, using Reynolds (Re) numbers 2,30 0 and 3,000 as the boundaries. To ensure smooth transitions, the frictional factor and HTC in the transitio nal flow region are interpolated based on the laminar and turbulent flow conditions.

The Python code considers friction, gravitation, and acceleration pressure drops in the hydrodynamic calc ulation. Python uses specific correlations for computing frictional factors in both single- and two-phase fl ows. In addition to calculations for the tube and shell side, the code also includes the thermal-hydraulic be havior of the riser section, which requires an additional loop to achieve consistent calculations.

2.1 Governing Equations and Correlations

Table 1 provides a list of the governing equations and correlations used in this work.

Table 1: Some governing equations and correlations.

Parameter	**Model/Correlation**	**Applicable Range**	**Reference**
Single-phase frictional factor		$0 < Re < 2300$	White [9]
			Petukhov et al. [10]
Two-phase fictional pressure drop			Lockhart and Martinelli [11]
Two-phase acceleration pressure drop			Todreas and Kazimi [12]
Two-phase gravitational pressure drop			Todreas and Kazimi [12]
Single-phase Nusselt Number			Incropera et al. [13]
			Gnielinski [14]
Sub-cooled boiling heat transfer rate			Chen [15]
Nucleate boiling heat transfer rate			Chen [15]

2.2 Reference Heat Exchanger Model

Figure 3 provides the plots showing SG pressure, thermodynamic quality, and temperature, as calculated via Python code. Preliminary results from both code outputs, as well as the data, exhibited similar trends.

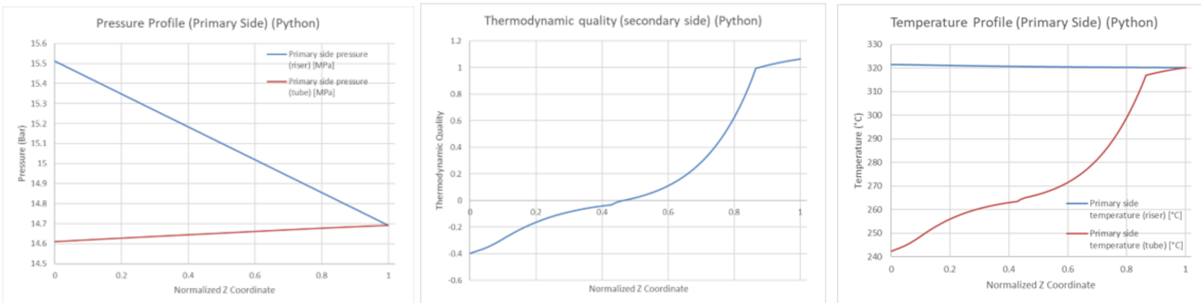

Figure 3: Plots output with the Python-based code.

3.0 PARAMETRIC STUDY

The parametric study assessed how the output of the code was impacted after changing all input parameters by either increasing or decreasing the percentages. This was done by running the Python SG code and changing the inputs in each run's input file. Each run then provided the SG data to compare against each other to view, in graphical terms, the impact of the changes with each output parameter being compared spatially against the SG length so that a localized analysis could be conducted.

3.1 Input/Output Parameters and their Ranges

The input parameters were HL/cold-leg (CL) inlet pressure, temperature, and mass flow rate (MFR). A specific range of accepted input values over which the correlations used in the code were viable are:

- HL pressure input: 5% below to 5% above the baseline
- HL temperature input: 0.2% below to 1% above the baseline
- HL MFR input: 2% below to 5% above the baseline
- CL pressure input: 1% below to 1% above the baseline
- CL temperature input: 5% below to 1% above the baseline
- CL MFR input: 3% below to 2% above the baseline.

Table 2 shows the baseline inputs for the parametric study.

Table 2: Baseline inputs for parametric study (values removed as they are proprietary information).

Baseline Inputs	Parameters
Primary side	Pressure (MPa), inlet temperature (K), and MFR (kg/s)
Secondary side	

The following output parameters were used: (a) tube/riser HTC, (b) primary-side pressure profile (riser and tube), (c) secondary-side pressure profile, (d) primary-side temperature profile (riser and tube), and (e) secondary-side temperature profile.

3.2 One-at-a-time Approach

The one-at-a-time approach, as outlined in Figure 4, bases the parametric analysis on a series of distinct steps that must be followed. Once the input and desired output parameters are identified, this method helps define a baseline set of input values that can vary and be compared against. The ranges were defined over which input parameters will vary, allowing the data output to slightly differ based on these changes. All six inputs were varied by increasing them in increments of 0.1–0.5%. This process can be repeated to see h ow the outputs change in accordance with the altered input, and should provide an in-depth review of the different outputs and how they were impacted by the various magnitudes of changes applied to the inputs.

Figure 4: One-at-a-time approach.

3.3 Results and Discussion

3.3.1 Influence of Input Changes on the HTC

The riser and tube HTCs vary as the input parameter values are increased from the baseline values in incr ements of 0.1%. On the riser side, little variation in the values was observed until about 40% of the SG le ngth, when the HTC began to fluctuate. For the baseline inputs, this fluctuation peaked at a normalized z-coordinate of around 0.52. At a 0.5% increase, the fluctuation occurred a little earlier at a normalized z-coordinate of around 0.44. This data shows that when all parameters are increased, the HTC begins to fl uctuate at different locations along the SG, as indicated in Figure 5.

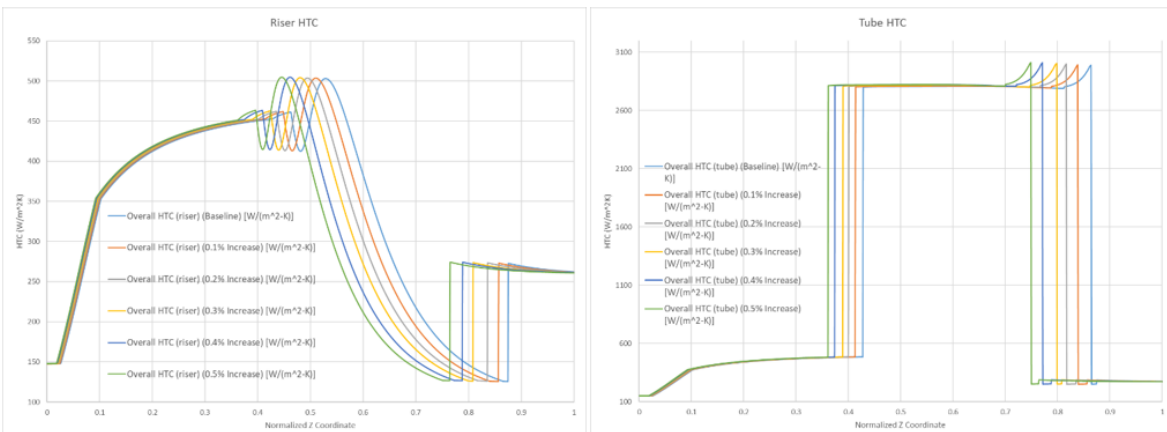

Figure 5: SG HTC under varied inputs.

A similar phenomenon was observed for the tube HTC, where the fluctuation reached its peak value at a n ormalized z-coordinate of 0.87 when using the baseline inputs. After a 0.5% increase, the peak HTC occu rred at a normalized z-coordinate of 0.75, while a slight increase in the peak HTC value as the input para meters increased was observed. This information is useful, as it indicates where properties of interest (e.g. , the HTC) reach their maximum. It also indicates how the HTC reacts to changed inputs. Most HTC valu e changes that occur with respect to increases in the input parameters take place in a specific SG region. O n both the riser and tube sides, this region is located somewhere between the normalized z-coordinates of around 0.3–0.9. This means that the HTC is most responsive to incremental changes made to the input par ameters along this section of the SG. Overall, the riser and tube HTCs are heavily impacted by input chan ges, as the peak HTCs take place at different locations. Furthermore, the tube HTC slightly increases as th e input values increase.

3.3.2 Influence of Input Changes on the SG Pressure Profile

The primary- and secondary-side pressures are also significantly affected by changes to the inputs, as seen in Figure 6. The primary-side riser pressure decreases as the normalized z-coordinate increases. As the in puts are increased incrementally, the initial and final riser pressures slightly increase, such that the slope i s the same as before, but with different intercepts. The primary-side tube pressure seems to follow a simil ar trend, except that, in this case, the pressure increases as the normalized z-coordinate increases. With ea ch small change in the inputs, again, only the intercepts of the pressure profile are observed to increase, whereas the slope remains constant. The secondary-side shell pressure decreases as the normalized z-coordinate increases. With each new run of the code generated, the pressure values become farther apart at a normalized z-coordinate of 0.4.

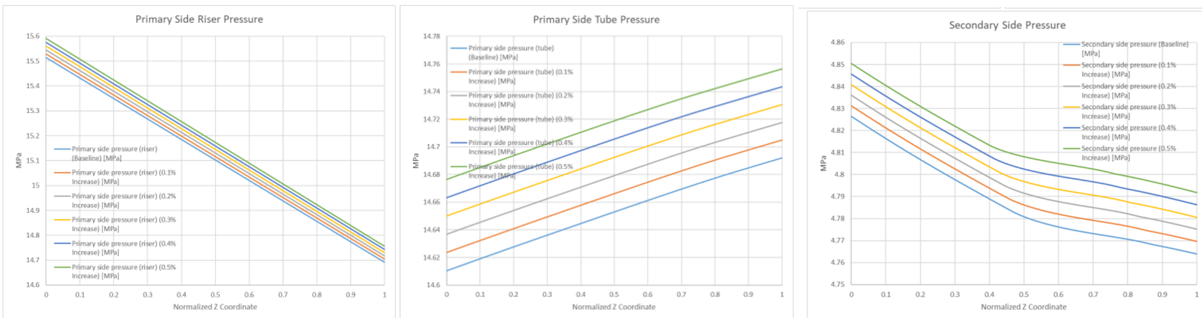

Figure 6: SG pressure profile under various inputs.

Overall, the pressure-based parametric study reveals the pressure increases as the inputs are increased. This increased pressure can be observed in the SG riser, tube, and shell. A 0.5% increase leads to an increase of around 0.1 MPa in the initial primary-side riser pressure, a 0.07 MPa increase in the initial primary-side tube pressure, and a 0.025 MPa increase in the initial secondary-side shell pressure.

3.3.3 Influence of Input Changes on the SG Temperature Profile

Figure 7 provides the results of the temperature-based parametric study, for the primary-side riser, primary-side tube, and secondary-side shell temperatures. The temperature in the primary-side riser section that reduces over the length is within 1.5 to 2.0 Δ°C. The temperature in the primary-side tube and secondary-side shell exhibited a gradual increase over the length in the bottom section of the SG model. The temperature increase in the middle section of the primary-side is sharp, whereas for the middle section of the secondary-side, the temperature is constant due to a boiling phenomena (i.e., latent heat transfer for phase change from liquid to steam). Temperature in the upper section of the primary-side tube and secondary-side shell increase slowly due to the lower HTC of steam in comparison to that of water.

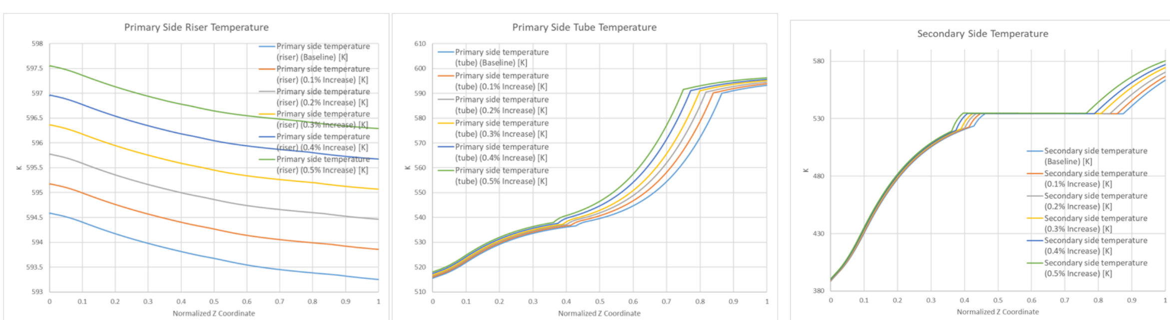

Figure 7: SG temperature profile under various inputs.

4.0 SENSITIVITY STUDY

A sensitivity analysis was performed on the SG design. Sensitivity analyses differ from parametric analyses in that they focus on how one specific input parameter affects the output as a whole, and each input is not varied a certain amount for each run. This analysis is conducted in two ways. First, by manually varying the input parameters to obtain the sensitivity data, with each input being assigned two different values within the given range in order to obtain the effect on the resulting output. The second part of the analysis uses RAVEN and its built-in techniques—paired with the Python code—to obtain AI-generated sensitivity data based on additional input perturbations, thus making the data more reliable. To perform a manual sen sitivity analysis, it is required to define the sensitivity coefficient, which is a value providing information on how significantly the input affects the output. A positive coefficient indicates that increasing the input should increase the output, while the magnitude of the coefficient tells us whether the input parameter has a great or a minimal effect on the output. The sensitivity coefficient can be calculated mathematically via many methods, the simplest being to divide the change in output by the change in input, as Equation (1):

(1)

To find the sensitivity coefficient of our inputs, the formula given in Equation (2) is used:

(2)

For example, to determine the sensitivity of the SG HTC to HL temperature, Equation (3) provides:

(3)

4.1 Parameters and their Ranges

For each interval along the vertical axis of the SG, the code calculates the pressure and temperature at that node. This means that each node has a specific spatial-based HTC value. For each node, this value will ch ange when the inputs are revised, thus providing new and initial HTC values usable for determining the se nsitivity at each node. This enables the ability to conduct a localized sensitivity analysis along the length of the SG for the various input parameters. Within the range of accepted values, two different values for e ach input are applied to investigate the sensitivity effects on the HTC output:

- HL pressure input: 5% below to 5% above the baseline
- HL temperature input: 0.2% below to 0.2% above the baseline
- HL MFR input: 2% below to 2% above the baseline
- CL pressure and temperature input: 1% below to 1% above the baseline
- CL MFR input: 2% below to 2% above the baseline.

4.2 RAVEN-Based Sensitivity Study

RAVEN is an machine learning platform developed by INL to process large amounts of data. It runs a co de multiple times, as decided by the user, and samples the data according to certain principles. The prelim inary case uses RAVEN to run the SG code 28 times, each time perturbing the inputs according to the Mo nte Carlo model, whereas the final sensitivity study considers 600 random samples. This allows us to hav e a large data set of HTCs for each perturbed input. RAVEN is used to find the sensitivity coefficients for each input on the HTC. It is important to note that the more perturbations RAVEN makes, the more accur ate the sensitivity data becomes. When doing the analysis manually, it takes a long time just to tweak the i nputs twice, as the Python code itself is computationally intensive and requires time to complete each run. Sensitivity data after running the code through RAVEN is much more accurate than the manual method, a s sampling is done randomly, and sensitivity coefficients can be averaged for overall accuracy. The range of perturbations for the Monte Carlo samples for the preliminary study was within ±0.2%, whereas the fin al revised study was within ±1% of the inputs to ensure the correlations in the code will not break down w hile running in RAVEN.

4.3 Results and Discussion

Manual perturbation of HL and CL inputs are performed independently to observe axial distribution of HTC in the primary-side tube and secondary side shell regions. Both HL and CL input perturbations considered changes on pressure, temperature, and MFR input. Results of the HTC based on HL inputs (i.e., pressure, temperature, and MFR) change/perturbation, which have similar trend with Figure 5 (for SG HTC for varied inputs). The results of HTC for the CL input change/perturbation also exhibited similar trend, therefore, not presented in this report.

4.3.1 Manual Perturbation Study of Hot-Leg Inputs

Temperature and MFR seemingly have a greater impact on the location of the maximum HTC. When these two parameters are increased, the maximum HTC moves closer toward the SG inlet, while a decrease brings the peak HTC closer to the outlet. The HTC reaction to pressure shows the opposite effect. As the pressure input is increased, the maximum HTC moves toward the outlet instead. It is also possible to gain a better understanding of the approximate sensitivity results obtained along the SG length. Under all parameters, sensitivity greatly increases within the 0.4–0.9 length region of the SG. Within this range, the tube MFR tends to impact the HTC most, with the riser MFR following closely behind. One additional observation is the inlet MFR has the greatest impact on the HTC in general, while inlet pressure has the least.

4.3.2 Manual Perturbation Study of Cold-Leg Inputs

Compared to the HL input, CL pressure has a greater impact on the maximum HTC location. In this case, MFR and temperature affect the HTC across the entire SG length, not just within the 0.4–0.9 normalized z-coordinate bounds. The HTC magnitudes, along with the location of the maximum HTC, are both affected by these changes. Another observation is that CL temperature has less of an impact on the HTC than HL temperature does, and increasing the CL MFR produces a larger HTC increase than increasing the HL MFR. The sensitivity across the SG length slightly increases for the tube MFR and tube temperature close to the SG inlet. The inlet parameters seemingly display a greater impact on tube conditions—as opposed to riser conditions—and thus, the impact occurs globally across the SG. CL temperature has the least impact on both the riser and the tube.

The preliminary results from the RAVEN analysis agree with the manual sensitivity study, with a range of sensitivity between 0.4–0.9 of the normalized z-coordinate. The values of the RAVEN-based preliminary sensitivity indicate the CL pressure has a significant impact on the tube HTC, while the HL temperature has a significant impact on the riser HTC. This differs from the manual results that show the MFR is the key influencing factor on the HTC. The RAVEN-based study takes 28 samples, while the manual study only takes two samples, requiring more detailed sensitivity studies.

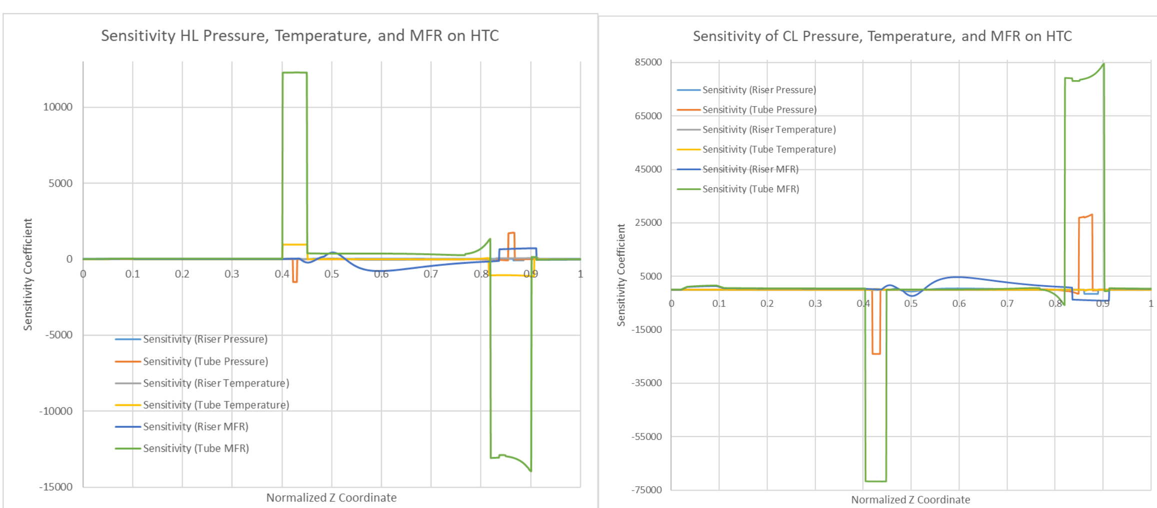

Figure 8: Preliminary sensitivity results on HTC along the SG length for the (a) HL input changes and (b) CL input changes. (Note: Here, x-axis is the normalized z coordinate).

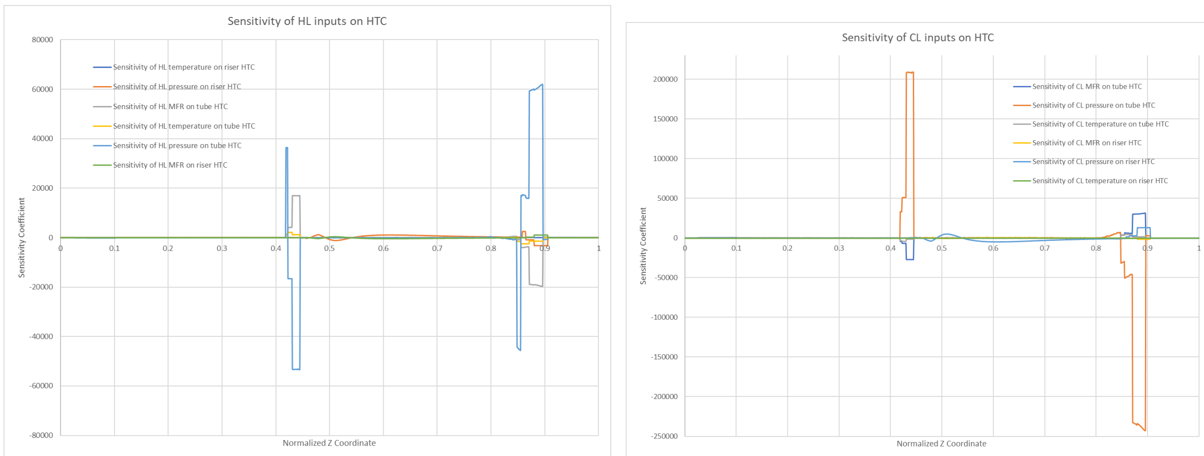

Figure 9: Preliminary RAVEN-based sensitivity results on HTC along the SG length for the (a) HL input changes and (b) CL input changes. (Note: Here, x-axis is the normalized z coordinate).

The preliminary sensitivity results were used to identify the exhibited entrance/exit effects on the riser top plenum region. An independent boundary case used for the top plenum region is needed to improve the S G design sensitivity and parametric studies. The revised sensitivity study results for 600 random samples using the Monte Carlo sampling method with RAVEN tools are provided in Figure 10. The samples are g enerated using uniform distributions (±1% relative changes) for the following input parameters: HL press ure input, HL temperature input, HL MFR input, CL pressure input, CL temperature input, and CL MFR i nput.

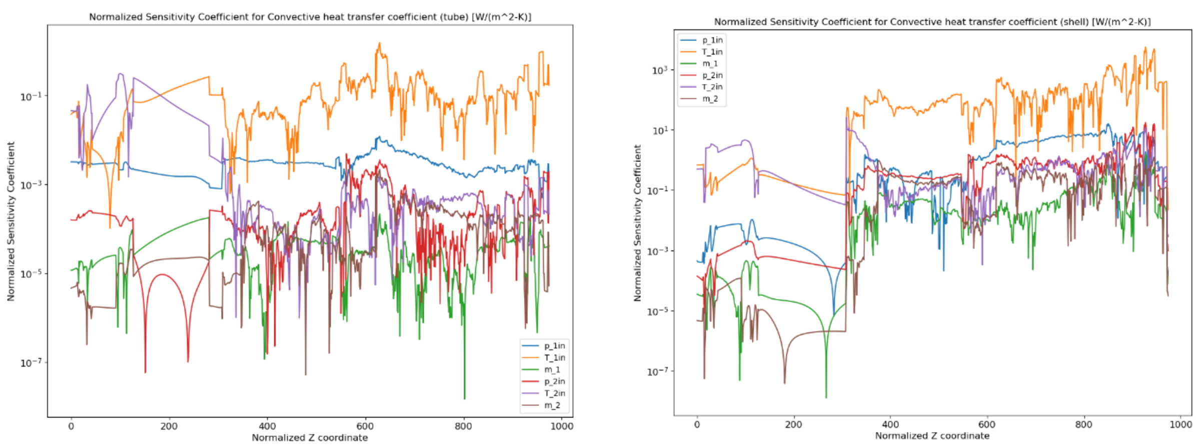

(a) **(b)**

Figure 10: RAVEN-based sensitivity results for the (a) tube side and (b) shell side. (Note: Here, x-ax is is the index for the normalized z coordinate)

5.0 CONCLUSIONS

Successful nuclear reactor system design and analysis requires various levels of qualifications for each sy stem, structure, and component, and interaction among them, for obtaining regulatory approvals. Among many components, the SG in a PWR-type SMR is considered as a lone component that interfaces between the primary and secondary coolant loops; therefore, SG design parametric and sensitivity study is pivotal. This study presented a specific reference for an SG model design parametric and sensitivity study. The ke y findings, observations, and recommendations are as follows:

- HL and CL temperature, pressure, and MFR have varied effects on the SG HTC. The impact of th e MFR on the HTC is greatest, followed by temperature and pressure. However, the RAVEN-bas ed results show that pressure and temperature also have a significant impact on the HTC—even m ore than the MFR. In the sensitivity analysis, the location of the maximum HTC was affected by i ncreasing or decreasing certain parameters.
- The preliminary parametric and sensitivity study exhibited the entrance and exit effect in the top plenum of the riser section required modification. Independent boundary cases were considered f or the riser top plenum region, which provided improved design data. The preliminary sensitivity study was only performed for 28 samples, which still implies the original manual sensitivity analy sis of the effect of temperature and pressure on the HTC is slightly skewed or inaccurate. The prel iminary sensitivity study shows the maximum sensitivity for all parameters falls within the 0.4–0. 9 normalized z-coordinate bounds, with certain parameters (e.g., CL temperature, MFR) having a more global impact on the HTC than others.
- The revised SG model shows the sensitivity ranges between 10^{-7} and 5×10^{-1} for the HTC, which provides greatly improved data than the preliminary design case.

6.0 ACKNOWLEDGEMENTS

The authors thank the United States (U.S.) Department of Energy (DOE) Science Undergraduate Laborat ory Internships (SULI), the Department of Nuclear Engineering at Purdue University, and the INL Therm al Fluid Systems Methods and Analysis for their support in this work.

7.0 REFERENCES

[1] International Atomic Energy Agency (IAEA), 2022, "Small Modular Reactors: A New Nuclear Energy Paradigm." IAEA, Vienna, Austria. Available at: https://nucleus.iaea.org/sites/smr/Shared%20Documents/Small%20Modular%20Reactors%20a%20new%20nuclear%20energy%20paradigm.pdf (last accessed 13 February 2023).

[2] Joshua P. Schlegel, P.K. Bhowmik, Chapter 14 – Small modular reactors, Editor(s): Jun Wang, Sola Talabi, Sama Bilbao y Leon, Nuclear Power Reactor Designs, Academic Press, 2024, Pages 283-308, ISBN 9780323998802, https://doi.org/10.1016/B978-0-323-99880-2.00014-X.

[3] Bhowmik, P. K., Perez, C. E. E., Fishler, J. D., Prieto, S. A. B., Reichow, I. D., Johnson, D. T., Sabharwall, P., and O'Brien, J. E., 2023. "Integral and Separate Effects Test Facilities to Support Water Cooled Small Modular Reactors: A Review." *Prog. Nucl. Energy* 160, 104697. https://doi.org/10.1016/j.pnucene.2023.104697.

[4] Holtec International, 2023. SMR-160, Camden, NJ, USA. https://holtecinternational.com/products-and-services/smr/, (accessed August 10, 2023).

[5] Park, Y., Kim, I., Kim, H., & Kang, K. (2021). "Development of a thermal-hydraulic analysis code for thermal sizing of once-through steam generators for SMR." *Progress in Nuclear Energy*, 139, 103883. https://doi.org/10.1016/j.pnucene.2021.103883.

[6] Rabiti C., Alfonsi, A., Cogliati, J., Mandelli, D., Kinoshita, R., Sen, S., Wang, C., Talbot, P. W., Maljovec, D. P., and Chen, J., 2017. "RAVEN User Manual. INL/EXT-15-34123, Rev. 6." *Idaho National Laboratory*, Idaho Falls, ID, USA. https://inldigitallibrary.inl.gov/sites/sti/sti/Sort_4450.pdf (accessed 6 February 2024).

[7] Karnik, N., Wang, C., Bhowmik, P. K., Cogliati, J. J., Balderrama Prieto, S. A., Xing, C., ... & Abdo, M. G. (2024). Leveraging Optimal Sparse Sensor Placement to Aggregate a Network of Digital Twins for Nuclear Subsystems. Energies, 17(13), 3355. https://doi.org/10.3390/en17133355.

[8] Bhowmik, P. K., Schlegel, J. P., Kalra, V., Mills, C., & Usman, S. (2021). Design of condensation heat transfer experiment to evaluate scaling distortion in small modular reactor safety analysis. Journal of Nuclear Engineering and Radiation Science, 7(3), 031406. https://doi.org/10.1115/1.4050211.

[9] White, F. M. (2011). *Fluid Mechanics (seventh edition)*. *McGraw-Hill*. https://www.academia.edu/36616285/Fluid_Mechanics_seventh_edition_by_Frank_M_White.

[10] Petukhov, B. S., Irvine, T. F., and Hartnett, J .P. (1970). *Advances in Heat Transfer*, Academic, New York, , 6, (1970): pp. 503-564.

[11] Lockhart, R. W. and Martinelli, R. C. (1949). "Proposed correlation of data for isothermal two-phase, two-component flow in pipes." *Chemical Engineering Progress*, 45, no. 1 (1949): pp. 39-48. http://dns2.asia.edu.tw/~ysho/YSHO-English/2000%20CE/PDF/Che%20Eng%20Pro45,%2039.pdf.

[12] Todreas, N. E. and Kazimi, M. S. (2021). "*Nuclear systems volume I: Thermal hydraulic fundamentals*." CRC Press.

[13] Incropera, F. P., et al. (2007). "*Fundamentals of Heat and Mass Transfer, 6th Edition.*" John Wiley & Sons.

[14] Gnielinski, V. (1976). "New equations for heat and mass transfer in turbulent pipe and channel flow." *International Chemical Engineering*, 16, no. 2 (1976): pp. 359-368.

[15] Chen, J. C. (1966). "Correlation for boiling heat transfer to saturated fluids in convective flow." *Ind Eng. Chem. Process Des. Dev.*, 5, no. 3 (1966): pp. 322-329. https://doi.org/10.1021/i260019a023.